Kite: Status of the External Metrology Testbed for SIM.

Frank G. Dekens, Oscar Alvarez-Salazar, Alireza Azizi, Steven Moser, Bijan Nemati, John Negron, Timothy Neville and Daniel Ryan.

Jet Propulsion Laboratory, California Institute of Technology
4800 Oak Grove Drive, Pasadena, California, U.S.A.;

ABSTRACT

Kite is a system level testbed for the External Metrology System of the Space Interferometry Mission (SIM). The External Metrology System is used to track the fiducials that are located at the centers of the interferometer's siderostats. The relative changes in their positions needs to be tracked to tens of picometers in order to correct for thermal deformations and attitude changes of the spacecraft. Because of the need for such high precision measurements, the Kite testbed was build to test both the metrology gauges and our ability to optically model the system at these levels. The Kite testbed is an over-constraint system where 6 lengths are measured, but only 5 are needed to determine the system. The agreement in the over-constrained length needs to be on the order of 140 pm for the SIM Wide-Angle observing scenario and 8 pm for the Narrow-Angle observing scenario. We demonstrate that we have met the Wide-Angle goal with our current setup. For the Narrow-Angle case, we have only reached the goal for on-axis observations. We describe the testbed improvements that have been made since our initial results, and outline the future Kite changes that will add further effects that SIM faces in order to make the testbed more SIM like.

Keywords: SIM, Metrology

1. INTRODUCTION

The External Metrology Sensor is needed to relate the base line changes between the guide and since interferometers of SIM.[1] It's duty is to correct for the fact that we are unable to keep a structure stable down to pico-meter levels. If we could do that, and articulate optics around a vertex defined to the picometer level, the External Metrology Sensor would not be needed. Since that's not feasible, we have to contend with more reasonable motions on the order of microns and instead measure the motions and correct for them. These motions are due to both temperature drifts and articulations of the siderostats. The External Metrology sensor itself has imperfections that cause nano-meter level effects, which in turn need to be corrected by using a ray-trace model in order to get down to the picometer level requirement.

The main components of the External Metrology System are fiducials, which define the baseline vectors, and metrology gauges, which measure the lengths between the fiducials. On SIM, there will be six fiducials. Four of these are double corner cubes, that is, they are back to back corner cubes with vertices of order ten microns apart; and they are located at the centers of the siderostats. Two of the fiducials are triple corner cubes, with vertices again of order ten microns apart; and these are

Further author information: (Send correspondence to F.G.D.)
F.G.D.: E-mail: fdekens@jpl.nasa.gov

located at the intersection of the guide-star light paths. In total, there are 19 gauges, where several of them are redundant, observing the fiducial-to-fiducial distances. This will form a 3D over-constrained system, which will be used to solve the fiducial motions. The motions will be handed over to the stellar interferometer as a correction to the delay line measurements. The Kite testbed is a 3 meter long planar version of such a metrology truss, placed inside a vacuum tank. Since there is no internal metrology, Kite only worries about self-consistency between the gauges. This 2D version has four fiducials measured by six gauges. The schematic layout of the testbed is shown in Fig. 1 . The testbed

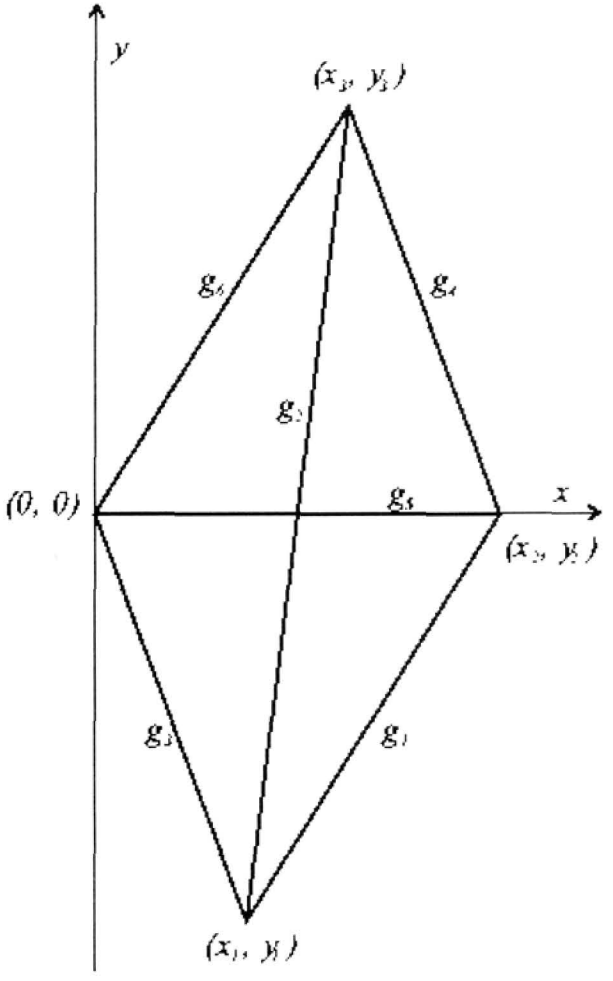

Figure 1. Schematic of the Kite layout. The actual system has a longer aspect ratio, but the scale has been changed to make the image more clear.

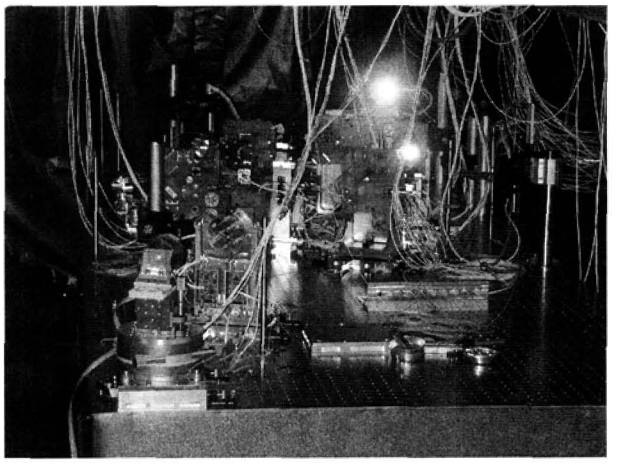

Figure 2. Image of the Kite testbed, taken from behind the PCC and facing the ACC. The brightest spot is the flash from the camera retro-reflecting inside the ACC corner cube. The bright spot to the lower right of it is the flash retro-reflecting from one of the corner cubes of the triples.

has been described in detail by B. Nemati.[?]

SIM has a Wide- and Narrow-Angle observing mode. We shall first describe the former. The Wide-Angle observing sequence is used for complete sky servays, which are done in a tile like fashion.

Each tile is fifteen degrees in diameter, during which the guide interferometers stay locked on the guide stars while the science interferometer articulates to the different target and reference stars. During this tile observation, the spacecraft is kept as stationary as possible. In between tiles, the spacecraft is articulated and new guide stars are acquired. The entire tile observing sequence is expected to take on the order of one hour. Kite therefor has an equivalent Wide-Angle observing scenario, where the ACC fiducial is articulated over an equivalent field. We show that sequence, the data and the latest results in Sec.

The Narrow-Angle mode is designed for targets of interest to which more time will be dedicated than in the Wide Angle case. Hence the target star is measured with respect to several reference stars. As much as 20 times more time is spend on a target as in the Wide-Angle case leading to significantly improved accuracy. We show Kite's equivalent measurement sequence and the results of our on-axis case in Sec. .

As mentioned earlier, Kite measures self consistency amongst the gauges. That is, we consider the longest length a base-line like quantity which in our case is actually measured directly by one of the gauges, namely Leg 2. We use the other five gauges to predict this length and then subtract the two. The algebra is straightforward and goes as follows. Following the schematic from Fig. , we place the coordinate system on the TCC-1 fiducial, with the X-axis going through the second fiducial. We label the fiducial coordinates as: $(x_0, y_0), (x_1, y_1), (x_2, y_2), (x_3, y_3)$ and the leg length as g_i, where i runs from 1 through 6. For convenience, we place our coordinate system at one of the triples: $(x_0, y_0) = (0, 0)$. By solving for the top and bottom triangles independently using the top and bottom lengths, we have:

$$(x_1, y_1) = \left(\frac{g_5^2 - g_1^2 + g_3^2}{2g_5}, -\sqrt{g_3^2 - x_1^2} \right) \quad (1)$$

$$(x_2, y_2) = (g_5, 0) \quad (2)$$

$$(x_3, y_3) = \left(\frac{g_5^2 - g_4^2 + g_6^2}{2g_5}, \sqrt{g_6^2 - x_3^2} \right) .. \quad (3)$$

From this, the predicted length between the top and bottom fiducials is just the distance equation: $g_2' = \sqrt{(x_1 - x_3)^2 + (y_1 - y_3)^2}$. The difference between the predicted and measured length is

$$\Delta \equiv g_2 - g_2' \quad (4)$$

. We typically refer to this as the "5-1" metric and will use in interchangeably with Δ.

Note that for all the above equations, the length is the absolute length. Our metrology gauges, however, are only capable of measuring relative motions. We therefor require a beginning step appropriately named "Absolute Metrology" mode, during which we switch between offset lasers in order to determine the absolute length down to the micron level. This data is shown in Sec. . Once we have established those lengths, we add it to the relative gauge measurements before calculating the metric. That is:

$$g_i = g_{i_{absolute}} + g_{i_{relative}} \quad (5)$$

for all legs i, where $g_{i_{absolute}}$ is the initial measurement of g_i, and $g_{i_{relative}}$ is the relative metrology measurement taken after some time. We show sample "relative" data Sec. , where we do not articulate the corner cube yet, but are tracking the thermal drifts of the testbed.

As Fig. shows, so far the articulating corner cube (ACC) is seen by all three relevant gauges. Because on SIM, the angles between the gauges is larger than the acceptance angle of a single corner

cube, SIM will need to use double corner cubes. We show future changes that will be made to the testbed to become more SIM-like and address additional errors that are caused by having multi-faceted corner cubes. That, along with our conclusions, is in Sec. 6.

2. ABSOLUTE METROLOGY

We will begin with the light source, since it is more complicated than the usual heterodyne source in that it is capable of switching between two lasers, which are locked to be 15 GHz apart. This is needed for absolute metrology measurement. SIM with have two of these for redundancy. A schematic is shown in Fig. 3 with an accompanying image in Fig. 4. The first set of acousto-optics modulators are

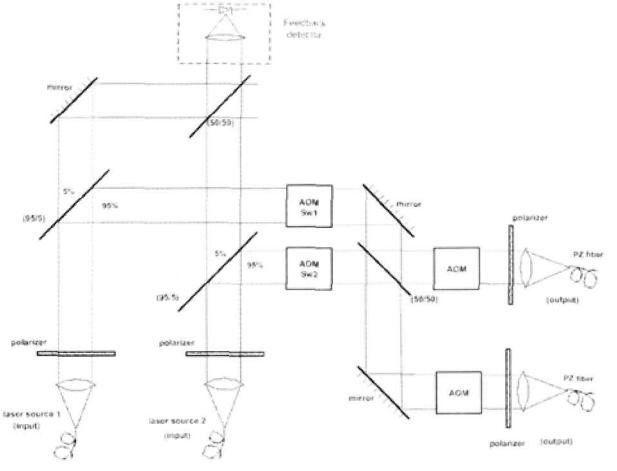

Figure 3. Schematic of the free-space source

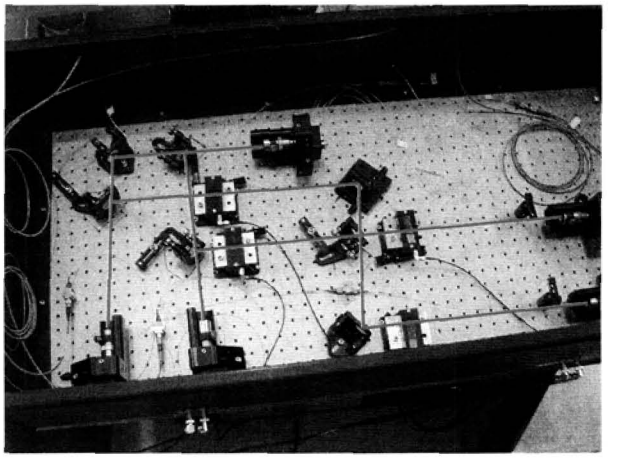

Figure 4. Image of the free-space source, where the red-lines are an overlay of the IR light-path.

there to quickly switch between two lasers, so only one of these is on at any given time. During regular (relative metrology) mode, we just use one of the lasers. During Abs. Met. these AOMs switch back and forward at 500 Hz. The remove the 200 μsec of data centered around that switch during which we loose lock of the 20 kHz heterodyne signal. This heterodyne signal is generated by the second, or right most, AOMs in the source. These two AOMs are always on and driven 20 kHz apart. Because we loose lock while switching the lasers, we only obtain the phase difference between the reference and measurement signals. This phase difference is measured for both lasers at 500 Hz each by switching between the two. A sample plot of the raw phases can be seen in Fig. 6 . From the difference in phase and knowing that the lasers are offset locked at $\delta\omega = 15$ GHz, we can calculate an absolute length to within an ambiguity length of 1 cm corner cube to corner cube (2 cm round trip). The equation used is $l = c\frac{\delta\phi}{\delta\omega}$, where c is the speed of light. The initial estimate, to within two centimeters was obtained using strings in the testbed which were then measured with a ruler. The calculated length for leg 1 is shown in Fig. 5. The mean of 1.571620 m has been subtracted in order to show the noise. This noise is again due to vibrations and averages out quickly. The RMS over ten minutes is typically a few microns. This is within the ten microns accuracy needed for Kite to obtain it's goal requirements. The largest error in our absolute metrology is due to amplitude sensitivity when converting the heterodyne signal to a phase measurement. The lengths of the Kite legs for the subsequent data was: 1.571615, 2.983117, 1.477939, 1.457499 0.534182 1.551161. The self-consistency error, calculated as in Eq. (4)

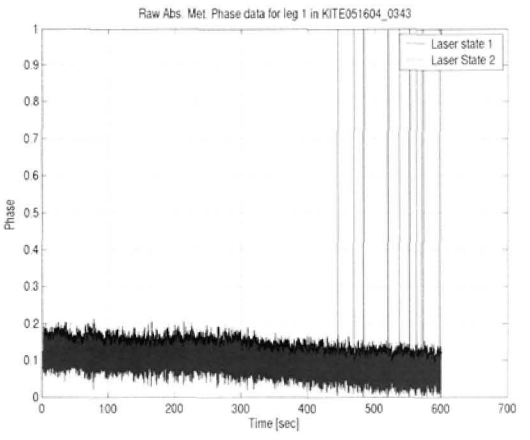

Figure 5. Sample phase data during an absolute metrology measurement. This shows the phases measured with the different lasers. The hash is due to vibrations of the ACC. Towards the end, the phase wrapping of the laser 2 state can be seen.

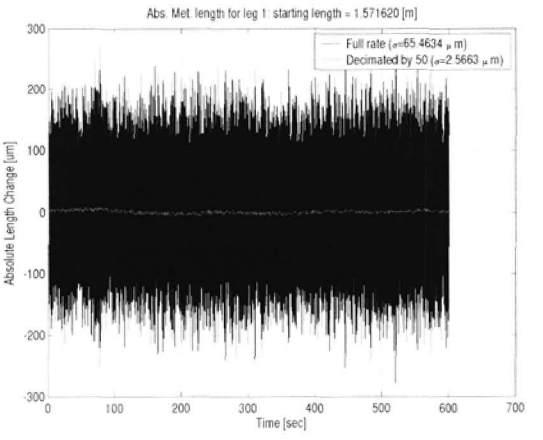

Figure 6. The same phases as in Fig. 6 were used to calculate the resultant absolute leg length.

but without adding relative gauge measurements is -14.8 microns. The RMS of the error sampled at 500 Hz for 10 minutes was 6 microns.

3. QUASI-STATIC

One of the more difficult problems in debugging Kite is that at the picometer level, nothing ever stays still. What we intend to be static is really just our most quiescent time and we label it as "Quasi-Static", because at least no corner cubes are articulating. It thus shows Kite's vibrations and drift noise floors. We only start taking data 2 days after the vacuum tank has been pumped down in order to minimize the thermal drifts. Sample data is shown in Fig. 7 , along with the Power Spectral Density if the same data in Fig. 8. The vibrations are much stronger in gauges 1, 2 and 3 because they each see the ACC. This corner cube is on a goniometer stack along with translation stages and has a forest of modes. Some of these modes are excited by the vacuum tank modes causing about 50 nm vibrations. This is of the order what is expected on flight, where the vibrations are required to be less then 10 nm RMS. These vibrations will be averaged out later during our stare times. When we add the absolute lengths to these relative measurements, we can calculate the "5-1" metric. This is plotted in Fig. 9 , again accompanied by its PSD of the same data in Fig. 10.

An other caveat that we have not touched upon yet is that the gauges need to properly point along the line connecting the two vertices of the fiducials. Because we need the gauges to point at the micro-radian level, we needed to have an active pointing system. The pointing error, however, is radially symmetrical and goes as $\delta l = lcos\theta$, where l is the length of the leg and θ is the pointing error. We therefor needed to dither the gauges in a circular fashion and essentially have a lock-in loop that looks at the amplitude and phase of the signal at the dither frequency. Furthermore, because we dither the entire gauge, they mechanically cross-talk. That is, dithering one gauge at frequency ν_{G1} causes the other gauges to see a signal at the frequency because they mechanically drive each other through the optics table. We therefor have slightly different dither frequencies for each gauge. Fig-X shows

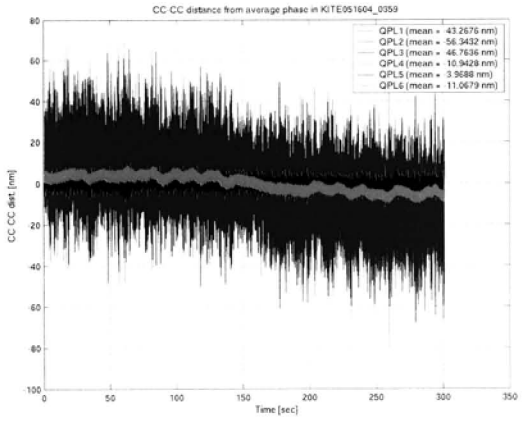

Figure 7. Quasi-Static data of the gauges.

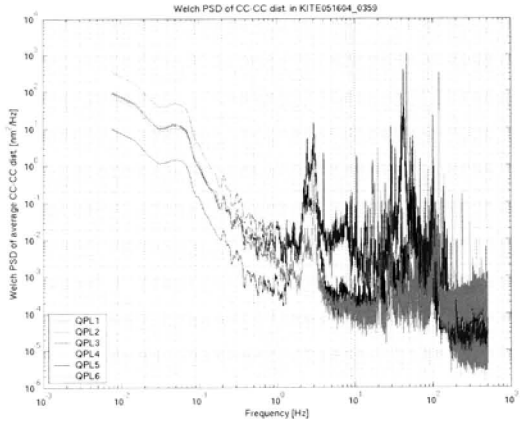

Figure 8. Power spectral densities of the gauge data.

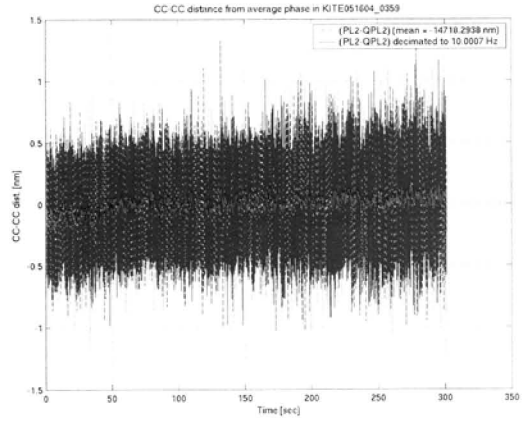

Figure 9. Calculated Δ as the difference between the predicted and measured length of leg 2.

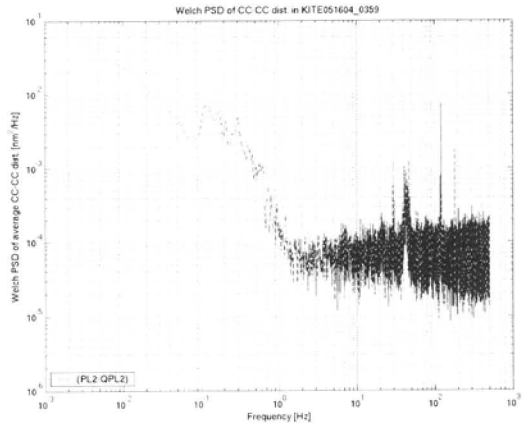

Figure 10. PSD of the Δ metric.

the power spectral density without the gauges dithering. There is a dip near 6 Hertz, which we use as the region to place the dithering frequency of the gauges. The full details of the filters and control algorithms are outside the scope of this paper and will be published at a later date.

4. WIDE ANGLE OBSERVING SCENARIO

Wide-Angle data on SIM consists of 15 degree wide tiles on the sky. That requires the science siderostats to articulate 3.75 degrees in radius to acquire the stars and hence so do the double corner cube fiducials that are located at the centers of the siderostats. For now, Kite only articulate one single corner cube. We have chosen a hexagonally symmetrical observing pattern with which we cover the tile. This pattern is shown in Fig. 11 . We start and end at the center of the field. For SIM this would be a reference start located near the center of the field. This way, we can remove linear temporal drift from the first to the last integration time or look, since they are the same observation. We made sure this would not

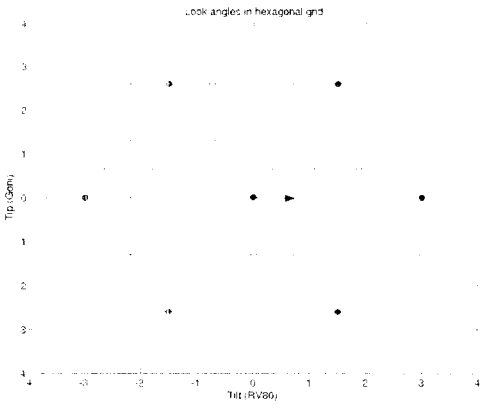

Figure 11. This shows the layout of the Kite WA grid. The corner cube first points at the center and starts by going to the right. After the right-most point, it goes up and to the left. It then follows the line until the pattern comes back on itself at the half way point, which is again in the center. It continues going right, but this time, when it gets to the right-most point, it now goes diagonally down and to the left. The pattern is then followed again until it arrives back at the center. This means that the 13 points along the y-axis are measured twice.

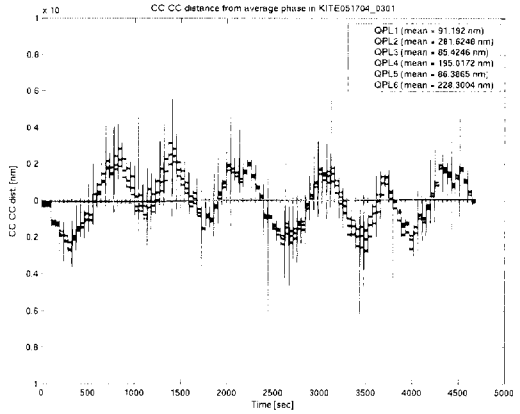

Figure 12. These are the measured lengths for the six gauges during the wide angle run versus time.

remove spatial information by having the hexagonal scan skip lines on the way up and then fill those lines in on the way back down. Positive tilt is pointing the ACC 1-1-1 axis more towards gauge 1, and positive tip is pointing the ACC 1-1-1 axis up out of the plane of Kite. We change the scanning pattern for some of the wide-angle data runs, so that we can distinguish true field dependent effects from other potential errors, such as source amplitude drift coupling into measurement errors or pointing errors.

During such a scan, the data is recorded for all six gauges at 100 Hz. A sample figure of the raw data is shown in Fig. . The large excitations are during the goniometer stack motions. The flat regions are where the 30 second looks are located. Also, there is some extra data at the beginning of each run that is used for diagnosing the pointing loops. From these relative gauge measurements, and using the most recent absolute metrology measurement, Δ is calculated, still at 100 Hz. This is shown in Fig. The "5-1" metric is now averaged down to 30 second averages. This timing is specified by SIM's predicted observing times. The resulting metric versus time is shows in Fig. . The first and last data points, marked with blue x's are used to calculate the drift. The green x's are linearly interpolated between the end points and get subtracted from the red x's which are the data. Note that for this file, the drift was slightly larger than 1 nm, which is typical. This is now ready to be plotted versus the angles of the ACC. Note that $(0, 0)$ is really just the starting point. For this particular file, the ACC 1-1-1 axis was pointed 11 degrees away from the line connecting the ACC to the PCC and towards gauge 1. First, in Fig. , we just show the Δ metric. This however, has a large field dependent plane. The second case, in Fig. , has the best fitted plane removed. Even after the plane has been removed, the residual RMS in the delta is xxx pm. Although this can get divided by $\sqrt{2}$

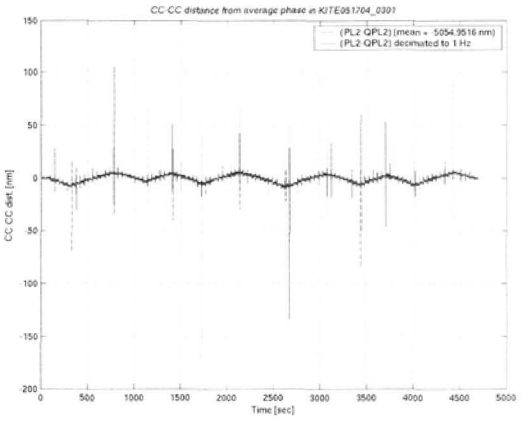

Figure 13. This is 5-1 metric for the wide angle run at 100 Hz. The large spikes are vibrations from the stepper motors while articulating the ACC. The quite times in between are the 30 second integration times.

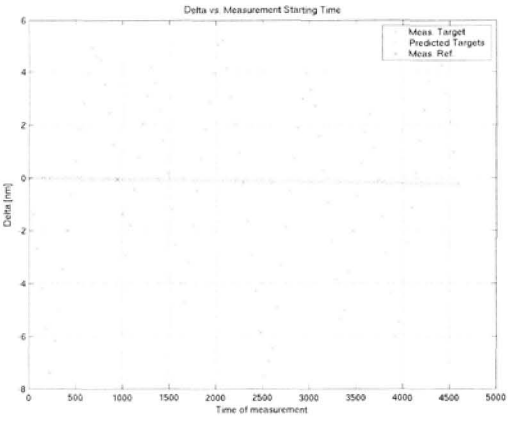

Figure 14. This is the average metric, where the averaging took place over 30 second.

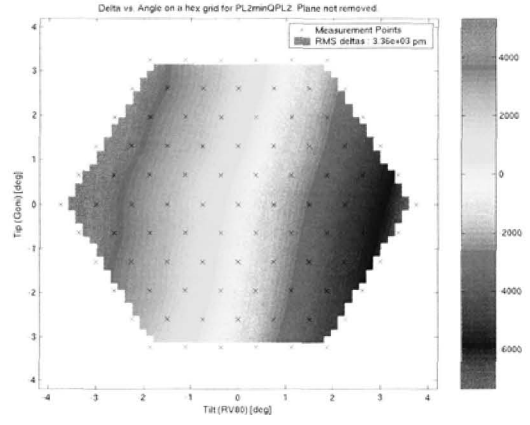

Figure 15. This is the wide angle field dependent surface. The prominent planer field dependence is due to dihedral errors in the corner cubes. That error effects the gauges differently causes a mismatch between the measured and predicted length

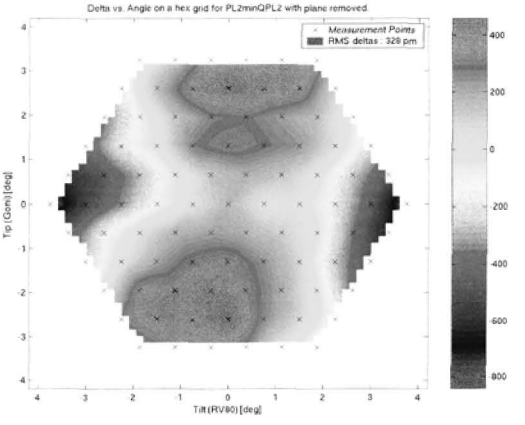

Figure 16. This is again the wide angle field dependent surface, but now the tip-tilt plane has been removed. The remaining dominant term is astigmatism caused by the gauges having different angles of reflection off the corner-cube surfaces. That causes different phase effects between the different gauges and in turn causes an error between the measurement and the prediction.

in order to obtain a per gauge error, rather than the "5-1" difference, it still does not get us to the 140 pm goal. A further necessary step is to generate a ray-trace model of Kite,[?] and generate a bias function which can be subtracted from the individual gauges before re-calculating Δ. The same data set, but with both the model and the best fit plane removed is shown in . This finally meets our goal

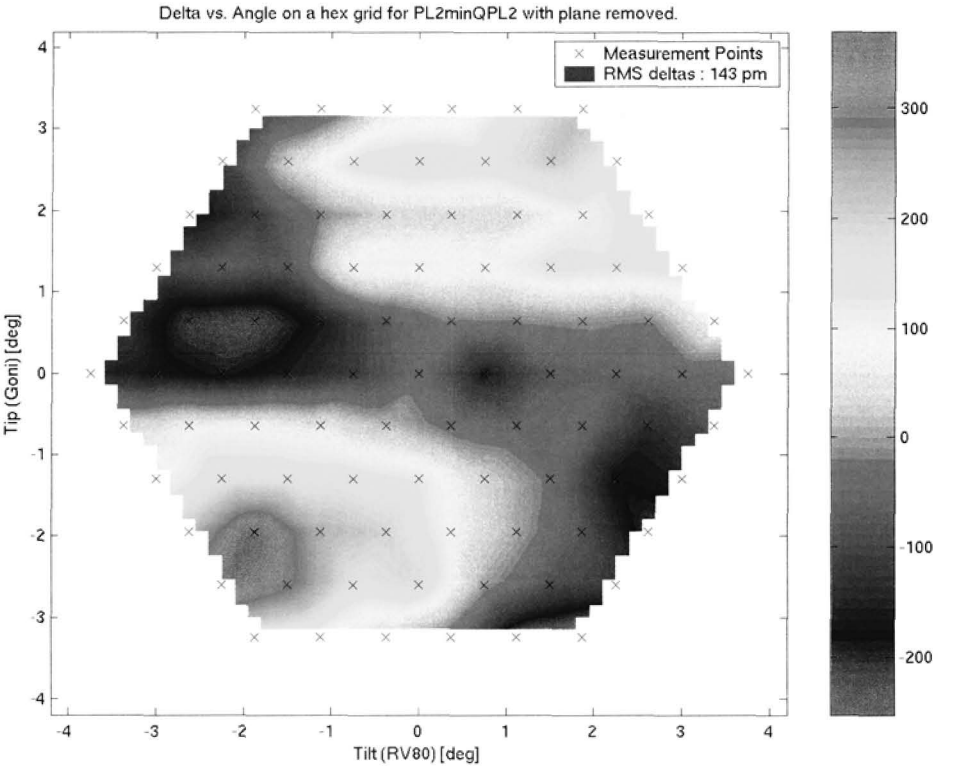

Figure 17. This is the same wide angle field dependent surface, but now both the model and the tip-tilt plane have been removed. The RMS over the averaged Δs is 143 pm. The per gauge error for this run is a factor of $\sqrt{2}$ lower, so 101 pm.

performance.

So far, we have only given one example data set. Because SIM will have gauges at various angles, we vary the starting angle of the ACC before starting the WA data run. The nominal cases as were the ACC 1-1-1 axis points towards the PCC. In that starting configuration, we also take data in a second scanning patter, where the X and Y axis are flipped. That makes the layout have a flip about the $tip = tilt$ axis. As in the above example, we also have cases where the ACC is first pointed 11 degrees towards gauge 1. We also take data where the ACC is pointed towards gauge 3 by 4 degrees. In all cases, we gain a great deal by having a model and without it Kite could not meet it's goal requirements. To gain a better understanding of which terms the model helps us in, we have fitted the field dependence surface to Zernike functions.[2] In Fig. 18 we show the Zernike coefficients fitted to this field dependent error for 18 data files. The first 5 files are the nominal type, the next five are taken with a different scanning pattern, the following 4 are tilted 11 degrees towards gauge 1 and the final 4 are tilted 4 degrees towards gauge 3. Note that for each change in the starting configuration — not for a change in scanning pattern – a different model and different bias function is generated. The fitted Zernikes after removing the appropriate model or bias function is in Fig. 19. The dominant change is of coarse in the tip and tilt. The second order terms are greatly improved too. This is particularly helpful because SIM can remove most of the linear term by fitting a plane across the field using reference starts. It is therefor the second order terms that we are most interested in. Once we

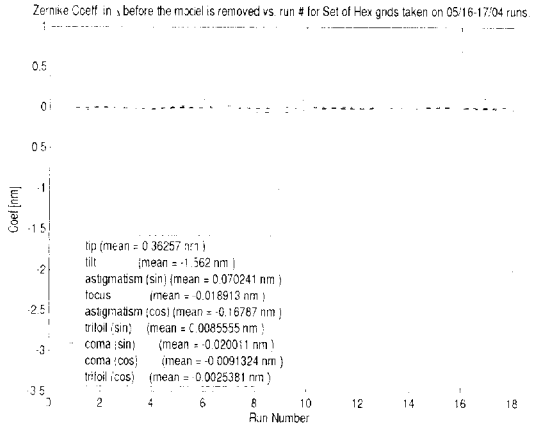

Figure 18. Fitted Zernike coefficients to the WA field dependent errors.

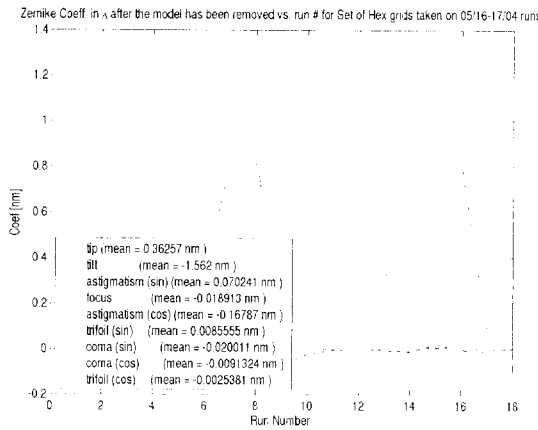

Figure 19. Fitted Zernike coefficients to the WA field dependent errors, but after the model has been subtracted.

remove the models, we can take all the observations and plot them in a histogram. This is done in Fig. , where we have also included the goal levels. The RMS of this distribution is 137 pm, which is just below the goal.

5. NARROW ANGLE OBSERVING SCENARIO

In the Narrow-Angle case, the emphasis switches to a single target star. Thus far, all the Narrow Angle work we have done on Kite has been towards getting the simplest case to meet the goal performance, which is only 8 pm of error per star and per gauge. For the simplest case, we take the target start to be at the center of the field and the ACC 1-1-1 axis is pointing towards the PCC. The target star gets measured with respect to four reference stars, each within 0.5 degrees from the target. Here the angle is on the sky, so again, we half that on Kite because the siderostat only need to articulate half the angle. As a start, we will take the four reference stars to be in the right, up, left and down positions. SIM is planning on having 10 chops per target star, where with a chop we mean the following: start with an integration of 15 seconds on the target star, then move towards a reference start during 15 seconds. There, average for 30 seconds before returning. Each chop ends with a final 15 seconds on the target star. The chop is then the reference measurement minus the average of the target measurements. That way, any linear temporal drift over the 90 seconds is removed. By repeating this over a symmetrical field, the linear field dependent terms drop out when averaging over all the directions. In Kite, each directions gets observed twice given a total of 8 chops that are averaged per target measurement. The 8 chop sequence is repeated 5 times during the course of 1 hours. We than reset the pointing loops, re-set all our metrology gauges, and repeat the sequence again. This is done for many hours and our best data set to date is shown in Fig. The single chops are shown and the field dependence can be seen. Note that the 6^{th} run was significantly noisier than the others due to some external disturbance affecting the pointing loops. For this data, each sequential set of 8 looks were averaged and the 8-chop averages are plotted in Fig. . Again 2 thick bars show the goal performance, which is 16 pm for the "5-1" metric. The factor of 2 between the Kite metric and the SIM error budget is due to two factors of $\sqrt{2}$. The first is because the error budget is per gauge and the "5-1" is the combined error in multiple

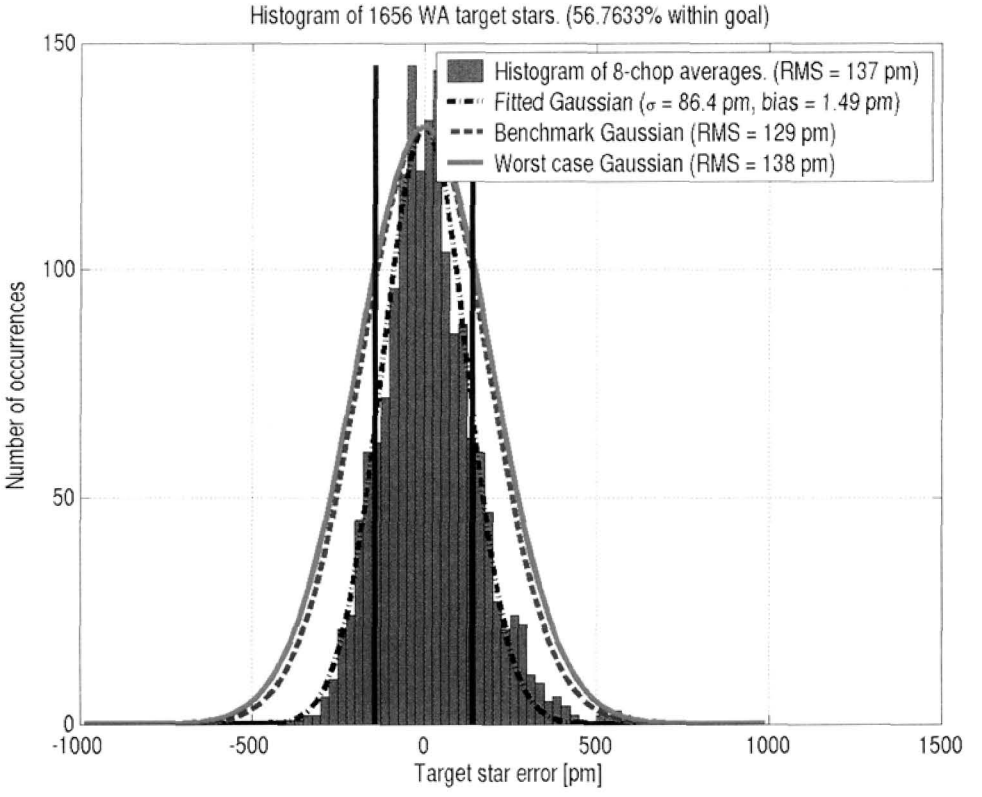

Figure 20. Histogram of the errors in the target measurements. The dark lines are at ± the Goal.

gauges. Because of the long aspect ratio of Kite however, the averaged error in the five other gauges has the same effective error as a single gauges. We consider the errors to be independent between the gauges and hence the first factor of $\sqrt{2}$. The second factor is because the error budget is in terms of a single star. We are measuring the difference between the target and reference stars however. Since we spend equal time on the reference stars and on the target, we again have equal errors between the two. The per star and per gauge equivalent error is on the right hand axis is Fig. 22. The histogram of the same data is show in Fig. 23, where the X-axis is again per gauge and per star. The resulting RMS of 10 hours worth of data and therefor 50 target star measurements was 5.6 pm. This shows our current electrical noise and isolation, our current optical crosstalk, pointing stability and vibration levels are all sufficiently low to start tackling the harder problems and start taking data off axis. As with the Wide-Angle, we will also need to remove a bias model for the off-axis data to be able to meet the goal performance.

6. CONCLUSION AND SUMMARY

The External Metrology System for SIM is a very complex sensor. Getting even the simplified Kite-shaped testbed with just four fiducials and six gauges to perform at the picometer level has been quite tedious and challenging. To obtain this performance a lot of improvements were needed since the original building of the testbed. Most of these were to obtaining both the stability and repeatability of the measurements along with needing to characterization testbed for modeling purposes. Meeting the

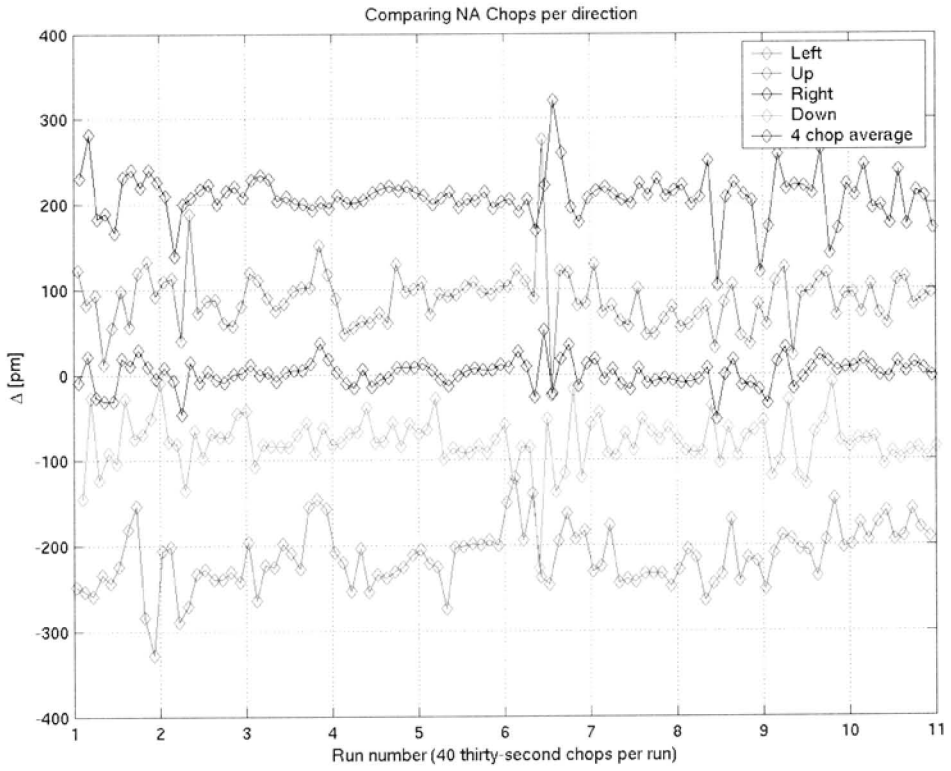

Figure 21. .

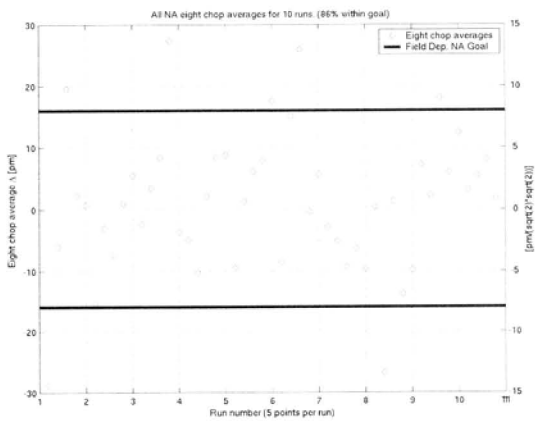

Figure 22. Summary of eight chop averages vs. time.

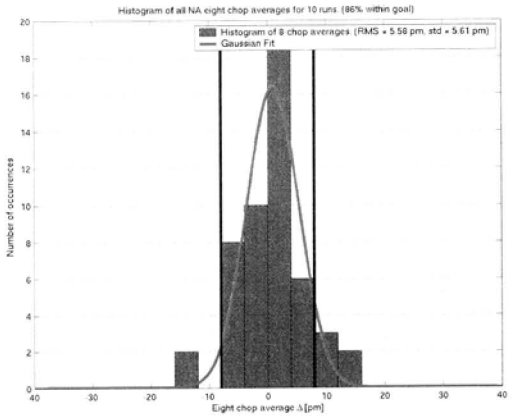

Figure 23. Histogram of 8 chop averages

stability required a more stable light source, mitigating ground loops in the electronics, improvements in the Absolute Metrology measurement techniques, and averaging optical cross-talk between the gauges. The repeatability has been challenging from the point of needing stable pointing loops and having the testbed automated enough to be capable of taking 10 to 20 hours of data without needing human

intervention. More accurate characterization of the testbed was needed than originally expected in order for the modeled bias functions to accurately remove the effects of both the dihedral effects of the corner cubes and the phase effects from the reflections of the bare gold surfaces.

We have demonstrated that, with the current Kite setup, we have reached a Wide-Angle per target RMS performance of 137 pm. This is just below the SIM goal of 140 pm. This was obtained over 18 data runs, each lasting 1.3 hours, with multiple scanning patters and multiple starting conditions of the articulating corner cube (ACC). The next step is to replace the corner cube, so that we can have more grazing angles of incidence. In the present Kite testbed, the largest angle of incidence between a gauge and the corner cube surface is 65 + 3.75 degrees. In the current SIM design (L19) the largest angle of incidence is 78 + 3.75 degrees. Once we have achieved goal level performance with more grazing angles of incidence, we will change the layout of the testbed and introduce double-corner-cubes, which will more accurately simulate the SIM optical truss. That final configuration will then contain the Non-Common Vertex Errors that are caused by having different gauges observe different fiducials. The different fiducials have different vertices that are on the order of 10 microns. Again a ray-trace model will be use do provide per gauge bias functions for Kite to meet it's goal performance. Once that is complete, the testbed will contain all the errors that the External Metrology System will have and we will demonstrate its ability to meet its allocated error in the SIM error budget.

In the Narrow-Angle observing scenario, we have reached a per-star per-gauge error of 5.6 pm. This is again below the SIM goal of 8 pm, but the data thus far is only on axis and without the bias model. The next step in NA is to go off-axis and meet the performance under multiple configurations and conditions. Once that it met, Narrow Angle will follow the same sequence in conditions as the Wide Angle case.

ACKNOWLEDGMENTS

This work was performed at the Jet Propulsion Laboratory, California Institute of Technology under contract with the National Aeronautics and Space Administration.

REFERENCES

1. R. Danner and e. Unwin S., eds., *Space Interferometry Mission, Takeing a Measure of the Universe*, JPL 400-811, 4800 Oak Grove Dr., Pasadena, Ca, U.S.A., 1999.
2. R. J. Noll, "Zernike polynomials and atmospheric turbulence," *J. Opt. Soc. Am.* **66**, pp. 207–211, Mar. 1976.